DESIGN STUDIES OF PROTON LINEAR ACCELERATORS*

D. E. Young, R. S. Christian, C. D. Curtis, T. W. Edwards, F. J. Kriegler, F. E. Mills, P. L. Morton, D. A. Swenson, J. van Bladel

MURA, USA

(Presented by D. E. YOUNG)

1. INTRODUCTION

Design studies of a 200 MeV conventional standing wave type of proton linear accelerator to be used as an injector for a 12.5 GeV FFAG accelerator have been carried out at MURA. The standing wave linear accelerator is limited in energy to about the value mentioned because of the decreasing efficiency of this structure at higher energies. However, because of the high efficiency at energies less than this, the ease of extraction, and the favorable external beam quality, the standing wave linac is receiving wide attention not only from synchrotron injector designers, but also from groups interested in continuing the linear acceleration with a change of cavity structure into the meson energy region. Groups known to be active in the design of standing wave proton linear accelerators of about this energy include groups at Brookhaven, Yale University, Los Alamos, Berkeley, Saclay, CERN, and Harwell.

In the last couple of years the art of design has been advanced by extensive use of digital computation techniques. At least two major problems are amenable to the computer approach. The first is an investigation of the radio-frequency structure. At MURA a program has been written which calculates the frequency and fields, and any other related quantity, from the geometry specified-arbitrary shaped drift tubes with holes are possible, but azimuthal symmetry is required. A similar program exists at Harwell [1] and other laboratories are writing or using such programs. The Yale group calculates resonant geometry, but in this case the fields are specified from charge distributions and the geometry is generated from the fields [2]. The second use of digital techniques is to study the particle dynamics in the linear accelerator. At MURA a program is in use which allows a large number of particles (500) to be simultaneously «flushed» through a linac which has previously been described to the computer in terms of accelerating fields, geometry drift spaces, and quadrupole focusing fields. Output can be obtained at any place along the linac so that it is possible to study the linac performance in terms of beam quality as the linac design is varied. This represents a powerful technique for studying the linac particle dynamics in the presence of the forces which couple the phase motion to the transverse motion. It provides a means for evaluating the fabrication tolerances, the effect of drift spaces between cavities, the problem of matching the linac injector into the linac, the optimum quadrupole focusing field strength, and many other aspects of linac design.

It appears that it is possible to design an adequate standing wave structure to accelerate particles to 200 MeV and to optimize the structure from the standpoint of cost. This optimization is based on the fact that, excluding fixed costs, the linac cost (including operating costs) can be broken down into costs per unit peak RF power and costs per unit length of accelerator. The cost of RF power for a given acceleration can be reduced by achieving a large value of ZT^2 of the cavity structure, where Z is the shunt impedance and T is the transit time factor. However, if ZT^2 is made large at the expense of the length of the cavity, that is to say, if a drift tube shape is chosen which is more likely to spark so that the acceleration rate must be decreased, the saving in power cost will be offset by the increased length cost. The sparking limit imposes a boundary condition on the maximum electric field in the cavity.

A few other design boundary conditions might be mentioned. The tank lengths are dictated by the power requirements which can be met by a single power amplifier tube. Sufficient reserve power must be available to allow compensation for beam loading and for

* Supported by the U. S. Atomic Energy Commission

Table 1

A 200 MeV Linear Accelerator Design

	Tank No. 1	Tank No. 2	Tank No. 3	Tank No. 4	Tank No. 5	Tank No. 6
Energy range (MeV)	0.75—10	10—53	53—95	95—132	132—167	167—200
Acceleration rate (MV/m)	1.7	1.7	1.7	1.6	1.4	1.3
Tank length (m)	5.5	25	24.5	23.5	24.5	25.5
Tank diameter (m)	0.94	0.94	0.92	0.88	0.86	0.84
Approximate drift tube diameter (cm)	19	19—13	15—14	18	19	19
Drift tube radius of curvature (cm)	—	4	4	6	6	6
Drift tube aperture diameter (cm)	2.5	3.0	3.5	4.0	4.5	4.5
Average shunt impedance (including transit time) (MΩ/m)	65	50	38	25	20	17
Cavity RF losses (MW)	0.3	1.8	2.3	3.0	3.0	3.1

practical cavity losses. At the same time the tank lengths cannot be so large that tank flattening is difficult, a restriction that prevents lengths of greater than 20 wavelengths. The drift tubes must not only be shaped to give a maximum ZT^2 and a maximum safe electric field close to 15 million volts per meter, but must allow radial focusing devices to be incorporated. The drift-tube holes must allow for the beam radial acceptance and for misalignments. A frequency of 200 MHz seems a good choice although this does impose difficult restrictions on the early drift tubes.

There is an obvious need for more experimental information to allow a practical design to be chosen, especially in the higher energy region. Cost savings should be possible by investigating new fabrication techniques in the cavities and drift tubes. The problems associated with the higher energy in the linac must be studied, especially with regard to exciting, tuning, and phase controlling the field, dissipating the increased power, and establishing better limits for the sparking levels. At the present time drift-tube stems and tuners which do not have azimuthal symmetry cannot be handled in the computing programs so that such frequency perturbations must be measured. There is a striking need for more and better instrumentation to allow a more informed tune up and operation to be achieved. With a many tank system it is no longer realistic to depend on simply knob turning to maximize the beam.

II. A 200 MeV LINAC DESIGN

Tables 1 and 2 illustrate a typical design of a 200 MeV linac broken down into tank lengths which can be powered by a 5 MW power stage and which are less than 20 wavelengths long. The geometry has been chosen using cylindrical shaped drift tubes although some advantage may be realized by using some other drift-tube shape. The average axial accelerating field has been chosen so that the peak electric field in any tank is conservatively below the limit imposed by sparking considerations.

Table 2

200 MeV Linear Accelerator Parameters

Tank resonant frequency	200 MHz
Stable phase angle	64°
Total accelerating length	128.5 m
Total RF peak power required (with beam loading)	24 MW
Average RF power at 1.2% duty factor	290 kW
Number of drift tubes	245
Maximum field strength at any point	less than 14 MV/m.

In this design special effort has been made to achieve a geometry (using cylindrically shaped drift tubes) which results in a cost minimum. By assesing both capital and operating power cost and capital and operating length costs, it is possible to evaluate the cost of the structure per MeV which stays within the limit imposed by sparking. In order to evaluate the structure in this way, it is necessary to have information for a broad range of the geometrical parameters, i. e., tank diameters, drift-tube shapes, gap lengths. Using the MURA field computational program, to be described in the next section, a large number of computer runs have been made for resonant geometry close to 200 MHz and at energies of 50, 100, 150, and 200 MeV, and with a smaller number of runs at 10 MeV intervals from

10 to 200 MeV. These runs give values for the transit time factor, the power efficiency measured in terms of the product of the shunt impedance and the square of the transit time

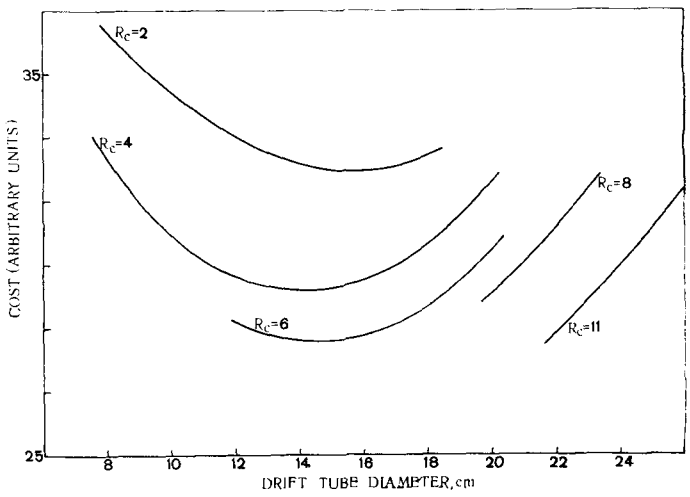

Fig. 1. A cost curve at 200 MeV for a tank diameter of 84 cm.

factor, and the peak field normalized unit average axial accelerating field. From this data, cost curves can be developed for any specified geometry. A respresentative set of curves is shown in Fig. I. This figure shows

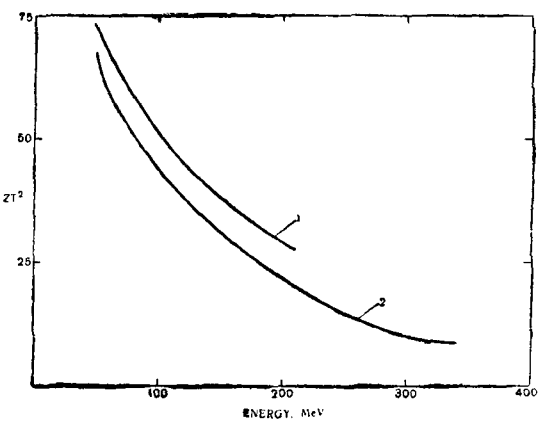

Fig. 2. ZT^2 as a function of energy for cylindrical and ellipsoidal drift tubes:
1 — ellipsoidal; *2* — cylindrical.

the cost of the structure as a function of the drift tube diameter for various radii of curvature on the corner of a cylindrical drift tube and at a constant tank diameter. For cylindrical drift tubes of small diameter, the values of both ZT^2 and the peak electric field are large. In order to offset the larger peak fields, the cavity excitation must be reduced, thus lowering the average accelerator rate and increasing the length of the linac, and the costs associated with length. When the hole is included in the drift tube, an obvious lower limit is imposed on the drift tube diameter. For the cost curves shown, the cost minimum at 200 MeV occurs for a cavity diameter of 84 cm and a drift-tube corner radius of 6 cm (for a 4.5 cm hole diameter with some curvature on the hole corner).

The cost minimum is quite broad allowing some flexibility in the drift tube design. Since our extensive study has included only the four energies mentioned, the design shown in Figs. 1 and 2 may not be considered optimum throughout even for a cylindrical drift-tube shape. Also the requirement of using a constant tank diameter may result in some departure from the optimum over the energy range covered by the tank.

III. FIELD COMPUTATIONS

The mathematical details of the MURA field computational program are given in the Appendix. The geometry of the unit cell is specified in terms of a tank diameter (D), unit cell length (L), gap length (g), and drift-tube contour. Cylindrical shaped drift tubes specified by a diameter (d), a corner radius (R_c), a hole diameter (a), and a hole corner radius (R_{HC}), have received the greatest attention, but other shapes are also possible. In particular, ellipsoidal drift tubes, specified by a major and minor axis and a hole diameter with a hole corner radius, have been selected to achieve higher power efficiencies than exhibited by the cylindrical shapes. A few more arbitrarily shaped drift tubes have been considered, but only a few computer runs have been made of these shapes.

Having specifield the geometry of the unit cell, the computer program calculates a resonant frequency and the fields at every point. From the fields it is not difficult to calculate the quantities of interest in linac design, namely, the power dissipated to the outer walls, the end plates, and the drift tube, the Q,

the shunt impedance, the transit time factor, or any other quantity based on these azimuthally symmetric fields. In particular, it is possible to search the metallic surfaces for the maximum electric field to see where sparking may occur and at what level. By renormalizing the fields to the maximum peak electric field considered «safe» from sparking considerations, the average axial accelerating field is found so that particle energy gain and the corresponding power dissipated can be calculated. This allows the geometry to be evaluated on a practical basis.

This program has been used to investigate the geometry at energies of 50, 100, 150, and 200 MeV for cylindrical drift tubes. Resonance curves have been developed which allow the tank diameter, drift-tube diameter, gap length, and drift-tube corner radius to be chosen for resonance at 200 MHz at these energies. Further, an examination of these runs allows one to make a selection of the geometry which will result in the largest power efficiency. Fig. 2 shows the maximum shunt impedance (including the transit time factor) plotted as a function of energy. It may not be possible to choose values this large in practice, however, since the hole size and the necessity to stay within the sparking limit without unduly increasing the linac length serve as restrictions. Shown in the same figure is a curve showing the possible gain in ZT^2 in going to an ellipsoidal shape for the drift tube. Again it is not claimed that the additional gain in ZT^2 for the ellipsoidal shape can be realized in practice. We have also considered drift tubes of other shapes, but no extensive study has been carried out for these cases and in fact appear to be undesirable from peak accelerating voltage considerations. At the present time nearly 1000 computer runs have been made at MURA for the type of geometry shown. These runs are now being summarized and published as an aid in the design of standing wave linear accelerators.

IV. PHASE AND RADIAL MOTION IN LINACS

We have prepared a computer program to trace the phase motions and the transverse motion of particles through a proton linear accelerator. The program is prepared to simulate a linac of standard design, namely a linac composed of a set of resonant linac cavities (tanks), each containing a series of drift tubes, each of which contains a quadrupole focusing magnet. The program proceeds by transforming the coordinates of a collection of particles through a set of transformations representing the linac. The transformations are chosen to represent Φ the important effects of the linac accelerating and focusing structure on the particles.

Each particle has six coordinates, namely x, x', y, y', E and Φ, where x, x', y and y' are the transverse displacements and angles of the particle trajectories in two transverse directions, E is the energy and Φ is the phase of the particle with respect to the RF accelerating voltage. If one ignores the coupling between the x, x' motion, the y, y' motion and the E, Φ motion, one can study each of the three motions independently. This has been done on many occasions, both analytically and digitally and is well described in the literature [3, 4, 5, 6]. It is extremely difficult to include the coupling between the transverse motion and the phase motion in the analytic approach. The present work is an attempt to study the effect of these coupling terms with the aid of digital computation.

In order to describe the nature of the coupling terms included in the program, we must outline the sequences of transformation performed by the program, and describe the functional dependence of each transformation. The linac is treated as a series of cells, each cell beginning at the center of one drift tube and ending at the center of the next. The main loop of the program transforms the coordinates of the particles through one cell.

The first transformation is denoted on the Fig. 3 as T1 and simulates the action of the quadrupole magnet on the transverse coordinates x, x', y and y'. The x, x' motion is independent of the y, y' and Φ coordinates, but is a function of the particle energy E. This transformation is one source of the coupling between the transverse motions and the phase motion. The second transformation is denoted on the slide as T2 and simulates a free-space drift to the electrical center of the accelerating gap. There are no coupling terms present here.

Before proceeding to the transformation T3 at the center of the gap, we shall dispense with transformation T4 and T5 by noting that they are similiar, except in magnitude, to transformations T2 and T1 respectively. The transformation T3 at the center of the

gap simulates the change in energy of the particle, and the net defocusing experienced by the particle on crossing the gap.

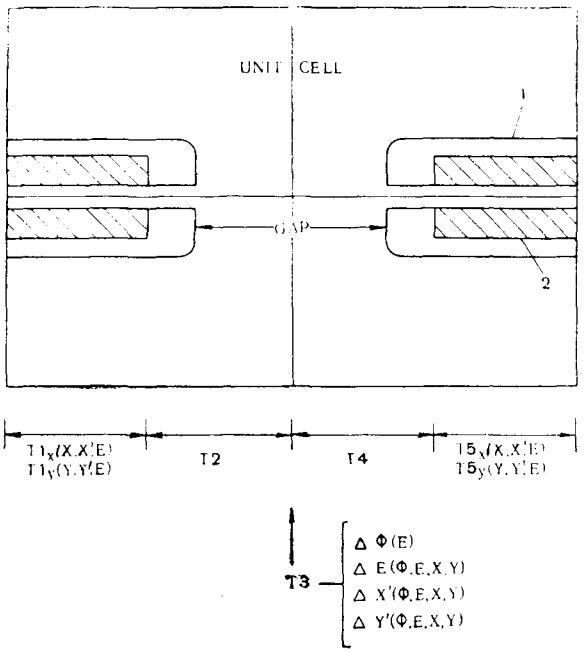

Fig. 3. Functional dependence of transformation: *1* — drift tube; *2* — quadrupole magnet.

The change in Φ from the previous gap is a simple function of the length of the cell and the longitudinal component of the particle velocity. The difference between the actual velocity, and the longitudinal component is a possible coupling between the phase motion and the transverse motion. This effect is very small and is ignored.

The change in energy on crossing the gap is a function of Φ and a longitudinal transit time function. The longitudinal transit time is a function of the particle energy E, and the effective length of the gap, which, in turn, is a function of the transverse coordinates x and y. Hence the change in energy is a function of Φ, E, x and y. This represents a strong coupling between the phase motion and the transverse motion. The defocusing action on the x' coordinate of a particle on crossing the gap is a function of Φ and x and a transverse transit time function, which is a function of E, x and y.

We are in the process of studying the admittance and emittance of specific linac structures with specific values for the quadrupole field strengths. From the same study will come information on nonadiabaticity of the phase motion in the low energy end of the linac. Many other aspects of linac design will be studied with this program.

V. CONCLUSION

The design of standing wave proton linear accelerators has been aided greatly in the last few years with the extensive use of digital computational techniques. Field computational programs allow a detailed investigation of the RF structure even to the extent of a cost optimization. Particle dynamics programs will yield better information and insight into particle behavior in linacs whose parameters can be readily adjusted. There is a need however for better experimental information, especially in the energy range above 50 MeV.

APPENDIX

Mathematical Procedures of the Field Computational Program

The calculation of electromagnetic eigenvectors and eigenvalues in linear accelerator-type cavities containing stemless drift tubes whose meridian plane cross sections are piecewise simply describable, can be accomplished by solving finite difference approximations to the wave equation[8]. The resulting eigenvectors and eigenvalues allow quantitative determination of relevant auxiliary electromagnetic quantities and of particle dynamic phenomena.

Maxwell's equations, when expressed in cylindrical coordinates, admit two linearly and azimuthally independent sets of solutions; one with a vanishing E_Φ, the other with a vanishing H_Φ (TM or TE modes, respectively). The former type of solution or mode has a nonvanishing E_z and hence permits an axial acceleration of particles, whereas the latter type does not.

Thus the modes of interest are the TM modes, for which:

$$E_z = \frac{i}{\omega\varepsilon}\frac{1}{r}\frac{\partial(rH_\Phi)}{\partial r}, \quad E_r = \frac{-i}{\omega\varepsilon}\frac{\partial(H_\Phi)}{\partial z}, \tag{1}$$

and

$$\frac{1}{r}\frac{\partial}{\partial r}\left(r\frac{\partial H_\Phi}{\partial r}\right)+\frac{\partial^2 H_\Phi}{\partial z^2}+\left(k^2-\frac{1}{r^2}\right)H_\Phi=0, \tag{2}$$

such that

$$k^2=\omega^2\mu\varepsilon=\frac{\omega^2}{c^2}=\left(\frac{2\pi}{\lambda}\right)^2. \tag{3}$$

The boundary condition applicable to the solution of Eq. (2) must be such that the tangential component of E vanishes on all metallic surfaces and

is expressable as:

$$\varepsilon \frac{\partial}{\partial t}(\hat{n} \times \bar{E}) = \hat{n} \times (\bar{\nabla} \times \bar{H}) = 0, \tag{4}$$

whereupon:

$$\hat{n} \cdot \bar{\nabla}(rH_\Phi) = \frac{\partial}{\partial n}(rH_\Phi) = 0. \tag{5}$$

Because of the comparative simplicity of the boundary condition, Eq. (5), it has been found advantageous to formulate the problem in terms of the dependent variable $F = rH\Phi$, whereupon the field components, Eq. (1), and the scalar wave equation, Eq. (2), become:

$$E_z = \frac{i}{\omega\varepsilon}\frac{1}{r}\frac{\partial F}{\partial r}, \qquad E_r = \frac{-i}{\omega\varepsilon}\frac{1}{r}\frac{\partial F}{\partial z}, \tag{6}$$

and

$$\frac{\partial^2 F}{\partial r^2} - \frac{1}{r}\frac{\partial F}{\partial r} + \frac{\partial^2 F}{\partial z^2} + k^2 F = 0. \tag{7}$$

At the onset of numerical solution of Eq. (7), subject to the boundary condition, Eq. (5), neither the eigenvector, F, nor the eigenvalue, k, are known. However, any «trial eigenvector» Φ, can always be expanded in terms of the true eigenvectors, Φ_n, in the form:

$$\Phi = \sum_n A_n \Phi_n, \text{ where } L\Phi_n + k^2\Phi_n = 0, \tag{8}$$

and where, in the present instance L is the operator indicated in Eq. (17). Upon manipulating the scalar product of Φ with $L\Phi$, the lowest eigenvalue k_1 can be expressed as:

$$k_1^2 \leqslant -\frac{\langle \Phi, L\Phi \rangle}{\langle \Phi, \Phi \rangle} = \frac{-\iint_s \frac{F}{r}\left[\frac{\partial^2 F}{\partial r^2} - \frac{1}{r}\frac{\partial F}{\partial r} + \frac{\partial^2 F}{\partial z^2}\right] dr\, dz}{\iint \frac{F^2}{r}\, dr\, dz}. \tag{9}$$

It is furthermore demonstrable that this leads to a variational principle, such that if Φ differs from the lowest eigenvector Φ_1 by a small amount proportional to a parameter λ, then the inequality of Eq. (9) is proportional to λ^2. This may be done by expanding the ratio of scalar products in a Taylor series and noting that the term proportional to λ vanishes, if the operator is self-adjoint, such that:

$$\frac{\langle \Phi, L\Phi \rangle}{\langle \Phi, \Phi \rangle} = \frac{\langle (\Phi_1 + \lambda\Psi), L(\Phi_1 + \lambda\Psi) \rangle}{\langle (\Phi_1 + \lambda\Psi), (\Phi_1 + \lambda\Psi) \rangle} = -k_1^2 + 0(\lambda^2). \tag{10}$$

Thus a convergent iterative process is realized if, alternatively, better «trial eigenvectors» Φ or F are chosen, and successively better eigenvalue approximations are calculated.

The calculation of improved trial eigenvectors may conveniently be accomplished by the technique of (over)relaxation. Upon constructing a cartesian two-dimensional array of discrete values of F at various r and z, the problem can be formulated as a «matrix» problem rather than the continuous problem expressed by Eq. (7). The fundamental equations, Eq. (7) and Eq. (9), may thus be written in finite difference form by expanding the various neighboring matrix elements about a central element F_{ij} via Taylor series. If only the four nearest neighbors of the central element F_{ij} are employed, the resulting approximations to Eq. (7) and Eq. (9), become, respectively:

$$F_{i,j+1}\left(1 - \frac{h}{2r_j}\right) + F_{i,j-1}\left(1 + \frac{h}{2r_j}\right) + F_{i+1,j} + F_{i-1,j} + (k^2h^2 - 4)F_{ij} + 0(h^4) = 0, \tag{11}$$

$$k_1^2 h^2 \simeq \frac{\sum_i \sum_j \left\{\frac{F_{ij}^n}{r_j}\left[F_{i,j+1}^n\left(1 - \frac{h}{2r_j}\right) + F_{i,j-1}^n\left(1 + \frac{h}{2r_j}\right) + F_{i+1,j}^n + F_{i-1,j}^n - 4F_{ij}^n\right]\right\}\Delta S_{ij}}{\sum_i \sum_j \frac{(F_{ij}^n)^2}{r_j}\Delta S_{ij}}, \tag{12}$$

where i and j are matrix indices referring to the z and r coordinates, respectively, and where h is the common interelement coordinate difference. The finite difference equation, Eq. (11), may be written as a Liebmann four-point algorism:

$$F_{ij}^{n+1} - F_{ij}^n = \alpha\left\{F_{ij}^n\left(\frac{k^2h^2}{4} - 1\right) + \frac{1}{4}\left[F_{i,j+1}^n\left(1 - \frac{h}{2r_j}\right) + F_{i,j-1}^{n+1}\left(1 + \frac{h}{2r_j}\right) + F_{i+1,j}^n + F_{i-1,j}^{n+1}\right]\right\}, \tag{13}$$

where it is assumed that the matrix is repetitively traversed in a regular manner, such that, upon improving F_{ij}^n into F_{ij}^{n+1}, the matrix elements $F_{i-1,j}^{n+1}$ and $F_{i,j-1}^{n+1}$ will have already been processed on the current $(n+1)^{\text{th}}$ traversal, whereas the matrix elements $F_{i,j+1}^n$ and $F_{i+1,j}^n$ are those remaining from the previous n^{th} traversal.

Note that the boundary condition given by Eq. (5) corresponds to a reflection effect which is easily applicable to all boundaries which coincide with a row or column of matrix elements. For example, $F_{i,j+1}^n$ can be replaced by $F_{i,j-1}^{n+1}$ in Eq. (13). However, for boundaries that are not parallel with a row or co-

lumn of matrix elements, such a procedure is not easily accomplished in applying the requisite boundary condition. For this latter case, an auxiliary «curvilinear matrix» can be constructed which follows the contour of the boundary and sufficiently overlaps the principal «rectangular matrix». The application of the houndary condition to this auxiliary matrix is then again easily accomplished by a reflection of the form indicated above.

The expressions analogous to Eqs. (13) and (12), for a curvilinear matrix element, are:

elements in Eq. (12) and in Eq. (15) are labeled with a superscript n signifies that each eigenvalue improvement should be deduced from those matrix elements which exist at the end of a traversal of all elements (done for the purpose of matrix element improvement).

In order to make full use of both the cartesian matrix and the curvilinear matrix, it is necessary to interpolate some matrix elements from one form of matrix to the other. Such interpolation formulae as are required may be deduced, for example, by expanding five matrix elements F_{ij} in two-dimensional

$$F_{lm}^{n+1} - F_{lm}^{n} = \alpha \left\{ F_{lm}^{n} \left[\frac{k^2}{\left(\frac{2}{h_\rho^2} + \frac{2}{h_\theta^2} \right)} - 1 \right] + \frac{1}{\left(\frac{2}{h_\rho^2} + \frac{2}{h_\theta^2} \right)} \left\{ F_{l+1,m}^{n} \left\{ \frac{1}{h_\rho^2} + \frac{1}{2h_\rho} \left[\frac{r_c}{\varrho (r_c + \varrho \sin\theta)} \right] \right\} + \right.\right.$$

$$+ F_{l-1,m}^{n+1} \left\{ \frac{1}{h_\rho^2} - \frac{1}{2h_\rho} \left[\frac{r_c}{\varrho (r_c + \varrho \sin\theta)} \right] \right\} + F_{l,m+1}^{n} \left\{ \frac{1}{h_\theta^2} - \frac{1}{2h_\theta} \left[\frac{\cos\theta}{(r_c + \varrho \sin\theta)} \right] \right\} +$$

$$\left.\left. + F_{l,m-1}^{n+1} \left\{ \frac{1}{h_\theta^2} + \frac{1}{2h_\theta} \left[\frac{\cos\theta}{(r_c + \varrho \sin\theta)} \right] \right\} \right] \right\}, \qquad (14)$$

and

$$\sum_l \sum_m \left\{ \frac{F_{lm}^{n}}{(r_c + \varrho \sin\theta)} \left[\frac{h^2}{h_\rho^2} (F_{l+1,m}^{n} + F_{l-1,m}^{n}) + \frac{h^2}{h_\theta^2} (F_{l,m+1}^{n} + F_{l,m-1}^{n}) + k_1^2 h^2 - \right.\right.$$

$$\left.\left. \frac{\left(\frac{h}{h_\rho} \right) \frac{(F_{l+1,m}^{n} - F_{l-1,m}^{n})}{2\left(\frac{\varrho}{r_c} \right)\left(\frac{r_c}{h} + \frac{\varrho}{h} \sin\theta \right)} + \left(\frac{h}{h_\theta} \right) \frac{\cos\theta \, (F_{l,m-1}^{n} - F_{l,m+1}^{n})}{2\left(\frac{r_c}{h} + \frac{\varrho}{h} \sin\theta \right)} - 2\left(\frac{h^2}{h_\rho^2} + \frac{h^2}{h_\theta^2} \right) F_{lm}^{n}}{\sum\sum_m \frac{(F_{lm}^{n})^2}{(r_c \varrho + \sin\theta)} \Delta s_{lm}} \right] \right\} \Delta S_{lm}, \qquad (15)$$

where ϱ is the (local) radius vector to the matrix element F_{lm} as defined in the curvilinear coordinate system, θ is the angle made by this radius vector with the axis of the cavity, r_c is the radial coordinate (in the cartesian system) of the (local) center of curvature associated with the matrix element F_{lm}, and h_ρ and h_θ are the radial and azimuthal interelement coordinate differences associated with the matrix element F_{lm}.

The factor α appearing in Eq. (13) and Eq. (14) is the overrelaxation factor. If $\alpha = 1$, these algorisms are rigorous. By judicious choice of $\alpha \geqslant 1$, however, accelerated convergence may be obtained. Although some attempts have been made to calculate the optimum value of α for algorisms derivable from Laplace's equation, little information has been found in connection with wave equations such as Eq. (7). Empirically, a value between approximately 1.4 and 1.9, increasing as the number of rectangular matrix elements increases from about 1000 to 8000, has been found best.

Further, the factors ΔS_{ij} and ΔS_{lm} appearing in Eq. (12) and Eq. (15) are meridian plane subareas required for the finite-difference integrations and associated with the various matrix elements F_{ij} and F_{lm}; whereas the fact that all of the various matrix

Taylor series about the matrix element F_{lm}, and requiring that a weighted sum of the five Taylor series be consistent with the fundamental identity, Eq. (7). This process leads, in this case, to:

$$F_{lm} = \sum_{u=1}^{5} \lambda_u (F_{ij})_u \Big/ \left(\sum_{u=1}^{5} \lambda_u - k^2 \right), \qquad (16)$$

where the λ's are the solutions of the indicated 5×5 matrix problem.

In practice, it is advantageous to use the best initial «trial eigenvector» available. Initially this may be done by using an analytic approximation, whereas, after a repertoire of solutions for geometries of interest has been developed, a reasonably good initial trial eigenvector may be obtained from a previously calculated solution.

The eigenvectors and eigenvalues so calculated may be used to compute several auxiliary electromagnetic quantities, including:

Energy Stored per Unit Volume:

$$\frac{W}{V} = \frac{\mu}{2} \frac{\int\int \frac{F^2}{r} \, dr \, dz}{\int\int r \, dr \, dz},$$

Power Lost to Cavity Walls:

$$P_w = \pi R_s \oint \frac{F^2}{r}\, dl,$$

Quality Factor:

$$Q = \frac{\omega\mu}{R_s} \frac{\int\int \frac{F^2}{r}\, dr\, dz}{\oint \frac{F^2}{r}\, dl},$$

Average Axial Accelerating Field:

$$\xi_0 = \frac{1}{\omega\varepsilon L} \int \left(\frac{1}{r}\frac{\partial F}{\partial r}\right)_{0,\,z} dz, \qquad (17)$$

Shunt Impedance:

$$Z_s = \xi_0^2/(P_w/L),$$

Transit Time Factor:

$$T = \frac{1}{\omega\varepsilon L \xi_0} \int \left(\frac{1}{r}\frac{\partial F}{\partial r}\right)_{0,\,z} \cos\frac{2\pi z}{L}\, dz,$$

Coupling Coefficient:

$$S = \frac{1}{\omega\varepsilon L^2 \xi_0} \int \left(\frac{1}{r}\frac{\partial F}{\partial r}\right)_{0,\,z} z \sin\frac{2\pi z}{L}\, dz.$$

It is convenient to normalize the eigenvector hus calculated, so as to permit easy comparison of results from similar geometry. This normalization may be carried out, for example, by requiring that the stored energy per unit volume or the average axial accelerating field remain constant. In this way relative figures of merit may be obtained from which the best geometry for a particular cavity energy, etc., may be determined.

REFERENCES

1. Taylor R. J. Nucl. Energy, Part C, 3, 123 (1961).
2. Gluckstern R. L. In: Proceedings of the International Conference on High Energy Accelerators (Brookhaven, 1961), p. 129.
3. Slater J. C. Rev. Mod. Phys., **20**, 473 (1948).
4. Blewett J. P. Internal BNL Report JPB-18, March 27, 1963.
5. Smith L. and Gluckstern R. L. Rev. Scient. Instrum., **26**, 220 (1955).
6. Cohen D. Internal ANL Report, ANLAD-57, July 16, 1959.
7. Van Bladel J. MURA Report No. 481, 1959 (unpublished).
8. Edwards T. W. MURA Report No. 622, 1961 (unpublished).